GEOPHYSICS, VOL. 56, NO. 10 (OCTOBER); P. 1650–1660, 7 FIGS.

Compensating finite-difference errors in 3-D migration and modeling

Zhiming Li*

ABSTRACT

One-pass three-dimensional (3-D) depth migration potentially offers more accurate imaging results than does conventional two-pass 3-D migration for variable velocity media. Conventional one-pass 3-D migration, using the method of finite-difference inline and crossline splitting, however, creates large errors in the image of complex structures. These errors are due to paraxial wave-equation approximation of the one-way wave equation, inline-crossline splitting, and finite-difference grid dispersion.

To compensate for these errors, and still preserve the efficiency of the conventional finite-difference splitting method, a phase-correction operator is derived by minimizing the difference between the ideal 3-D migration (or modeling) and the actual, conventional 3-D migration (or modeling). For frequency-space 3-D finite-difference migration and modeling, the compensation operator is implemented using either the phase-shift, or phase-shift-plus-interpolation method, depending on the extent of lateral velocity variations. The compensation operator increases the accuracy of handling steep dips, suppresses the inline and crossline splitting error, and reduces finite-difference grid dispersions.

INTRODUCTION

One-pass, as opposed to two-pass, 3-D wave-equation migration has been advocated for imaging common-midpoint (CMP) stacked 3-D seismic data, primarily where velocity varies both vertically and laterally (Yilmaz, 1987). Finite-difference implementations of one-pass 3-D migration often use the inline (x) and crossline (y) splitting technique in each step of wavefield extrapolation (Brown, 1983). While the splitting technique affords computational efficiency, known errors in positioning steeply dipping reflectors result, especially when the $x-$ and $y-$ directions are far from the dominant strike-dip direction.

Many approaches have been taken in the past 10 years to overcome this problem. Ristow (1980) suggested further splitting along the two diagonal directions ($x = \pm y$), besides splitting along x and y in each downward extrapolation step. Kitchenside (1988) used the method of phase-shift migration plus finite-difference residual wavefield extrapolation to reduce the error due to splitting. Graves and Clayton (1990) proposed implementing a phase-correction operator using finite-differences with a damping function (to ensure stability) in their 3-D paraxial wave-equation modeling of seismic wavefield. Hale (1990) proposed a 3-D, explicit finite-difference migration using McClellan transformations as an alternative to x–y splitting.

Instead of using phase-shift migration plus finite-difference residual wavefield extrapolation as in Kitchenside's approach, I use the conventional finite-difference migration plus phase-shift residual wavefield extrapolation to improve accuracy. Without any changes to the existing conventional one-pass 3-D implicit finite-difference migration, I simply add the error compensation as a phase-shift filter at certain steps of downward extrapolation. The method presented in this paper compensates not only for the splitting error, but also for steep-dip positioning error, and finite-difference dispersion error. This is done by using Gazdag's (1978) method of phase shift, but instead of using the wave equation, I use what I call the *finite-difference-error compensation equation*. In the presence of strong lateral velocity variations, again, the Gazdag's method of phase shift plus interpolation (Gazdag and Sguazzero, 1984) is used to implement the finite-difference-error compensation equation.

PARAXIAL EQUATIONS AND INLINE-CROSSLINE SPLITTING

The 3-D acoustic wave equation for upcoming waves in the frequency-space domain (ω, x, y, z), neglecting spatial derivatives of velocity, can be written as,

Manuscript received by the Editor September 18, 1990; revised manuscript received March 15, 1991.
*Formerly Center for Wave Phenomena, Colorado School of Mines, Golden, CO; presently Unocal La Palma Center, 5460 East La Palma Ave., P.O. Box 68076, Anaheim, CA 92817.

$$\frac{\partial P}{\partial z} = \frac{i\omega}{v(x, y, z)} \sqrt{1 + \frac{v^2(x, y, z)}{\omega^2}\left(\frac{\partial^2}{\partial x^2} + \frac{\partial^2}{\partial y^2}\right)}\, P, \tag{1}$$

where $P = P(\omega, x, y, z)$ is the wavefield, ω is radial frequency, x is the lateral coordinate along the inline direction, y is the lateral coordinate along the crossline direction, z is depth, and $v(x, y, z)$ is velocity.

To solve equation (1) numerically in the (ω, x, y, z) domain, the square-root operator must be expanded and approximated with a certain order of paraxial equation, depending on the accuracy of approximation. Using the continued fractions expansion (Claerbout, 1985) of the square-root operator and factorization of the expansion (Ma, 1982), equation (1) can be approximated with the following paraxial equation of order $2n$, again neglecting the spatial derivatives of v,

$$\frac{\partial P}{\partial z} = \frac{i\omega}{v(x, y, z)} \left[1 + \sum_{i=1}^{n} \frac{\alpha_i S}{1 + \beta_i S}\right] P, \tag{2}$$

where α_i and β_i are expansion coefficients given by Lee and Suh (1985), $S = S_x + S_y$ and $S_x = (v^2(x, y, z)/\omega^2)\partial^2/\partial x^2$, $S_y = (v^2(x, y, z)/\omega^2)\partial^2/\partial y^2$.

The higher the order $2n$, the better equation (2) approximates equation (1) in handling steep dips. In practice, the paraxial equation with $n = 1$ yields good accuracy for dips up to 65 degrees (Yilmaz, 1987). Equation (2) can be solved using a splitting method, resulting in the following sequence of $(n + 1)$ equations,

$$\frac{\partial P_0}{\partial z} = \frac{i\omega}{v(x, y, z)} P_0, \tag{3}$$

$$\frac{\partial P_1}{\partial z} = \frac{i\omega}{v(x, y, z)} \frac{\alpha_1 S}{(1 + \beta_1 S)} P_1,$$

$$\frac{\partial P_2}{\partial z} = \frac{i\omega}{v(x, y, z)} \frac{\alpha_2 S}{(1 + \beta_2 S)} P_2,$$

$$\vdots$$

$$\frac{\partial P_n}{\partial z} = \frac{i\omega}{v(x, y, z)} \frac{\alpha_n S}{(1 + \beta_n S)} P_n,$$

with $P_i(\omega, x, y, z) = P_{i-1}(\omega, x, y, z + dz)$, $i = 1, 2, \ldots, n$; $P_0(\omega, x, y, z) = P(\omega, x, y, z)$, and $P(\omega, x, y, z + dz) = P_n(\omega, x, y, z + dz)$.

Migration or modeling involves extrapolation of the wavefield using equation (1). Therefore, when using the splitting method, one needs to solve the above $(n + 1)$ equations in each step of extrapolation. The solution of each equation in (3) is used as a boundary condition to solve for the next equation in (3), until all $(n + 1)$ equations are solved for any single step of wavefield extrapolation. Solving the first equation in (3) is simply a multiplication of the wavefield P by a phase-shift operator $\exp(i\omega/v(x, y, z))$.

The last n equations in (3) all have the same form but with different constant coefficients α_i and β_i. Let's examine a representative numerical solution to one of them.

$$\frac{\partial P_k}{\partial z} = \frac{i\omega}{v(x, y, z)} \frac{\alpha_k S}{(1 + \beta_k S)} P_k. \tag{4}$$

In the ω-x-y domain, *implicit* finite-difference schemes are usually used to solve the paraxial wave equation because of their unconditional numerical stability (Claerbout, 1985). However, direct solution of equation (4) by an implicit finite-difference scheme will require solving a large $(nx \cdot ny \times nx \cdot ny)$ sparse-matrix equation, with enormous computational effort (Claerbout, 1985). A more practical but less accurate method is to use further splitting of equation (4) along inline x and crossline y directions (Brown, 1983). That is, instead of solving equation (4) in each step of extrapolation, we solve successively

$$\frac{\partial P_k}{\partial z} = \frac{i\omega}{v(x, y, z)} \frac{\alpha_k S_x}{(1 + \beta_k S_x)} P_k, \tag{5}$$

$$\frac{\partial P_k}{\partial z} = \frac{i\omega}{v(x, y, z)} \frac{\alpha_k S_y}{(1 + \beta_k S_y)} P_k.$$

Using an implicit finite-difference scheme, we then solve a $(nx \times nx)$ matrix equation for different y's (difference lines) and then solve for a $(ny \times ny)$ matrix equation for different x's (difference CMP positions). The computational count in doing so is proportional to $nx \times ny$, a significant reduction from the direct solution method (i.e., without the x-y splitting). The approximations made in the x-y splitting method, i.e., $S_x S_y$ small and S_x and S_y commutable, however, will cause significant errors in handling steep dips, especially along diagonal lines $x = \pm y$, as analyzed in the next section.

ERROR ANALYSIS AND COMPENSATION

Equation (5) is obtained by first approximating equation (4) with the following differential equation,

$$\frac{\partial P_k}{\partial z} \approx \frac{i\omega}{v(x, y, z)} \frac{\alpha_k(S_x + S_y) + 2\alpha_k\beta_k S_x S_y}{1 + \beta_k(S_x + S_y) + \beta_k^2 S_x S_y} P_k$$

$$= \frac{i\omega}{v(x, y, z)} \frac{\alpha_k S_x}{(1 + \beta_k S_x)} P_k + \frac{i\omega}{v(x, y, z)} \frac{\alpha_k S_y}{(1 + \beta_k S_y)} P_k, \tag{6}$$

and then splitting to separate the x-dependent and y-dependent operators. The approximation is valid only if $S_x S_y$ is zero or sufficiently small.

Substituting equation (6) (with corresponding α_i and β_i) for the second, the third, . . . , and the last equations in (3), we recognize that the exact equation (1) is actually replaced with the following approximate equation,

$$\frac{\partial P}{\partial z} = \frac{i\omega}{v(x, y, z)} \left[1 + \sum_{i=1}^{n} \frac{\alpha_i S_x}{1 + \beta_i S_x} + \sum_{i=1}^{n} \frac{\alpha_i S_y}{1 + \beta_i S_y}\right] P. \tag{7}$$

The finite-difference error E is defined as the difference between the original single square-root operator and the sum of the two split finite-difference operators plus 1, given below as,

$$E = \sqrt{1 + S_x + S_y} - \left[1 + \sum_{i=1}^{n} \frac{\alpha_i S_x}{1 + \beta_i S_x} + \sum_{i=1}^{n} \frac{\alpha_i S_y}{1 + \beta_i S_y} \right]. \quad (8)$$

As explained later in this section, E is the timing error (in seconds) created per second of downward extrapolation via the finite-difference method. Given the dip angle (θ) of reflector and the inline azimuth angle (ϕ) (the angle between the x-axis and the dip direction of the reflector) as shown in Figure 1, one can extend the S_x-θ relation for 2-D data (Claerbout, 1985) to obtain the (S_x, S_y)-(θ, ϕ) relation for 3-D data,

$$S_x = -(\cos\phi \cdot \sin\theta)^2, \qquad S_y = -(\sin\phi \cdot \sin\theta)^2. \quad (9)$$

Therefore, E can be rewritten as,

$$E = \sqrt{1 - \cos^2\phi \sin^2\theta - \sin^2\phi \sin^2\theta} - \left(1 - \sum_{i=1}^{n} \frac{\alpha_i \cos^2\phi \sin^2\theta}{1 - \beta_i \cos^2\phi \sin^2\theta} - \sum_{i=1}^{n} \frac{\alpha_i \sin^2\phi \sin^2\theta}{1 - \beta_i \sin^2\phi \sin^2\theta} \right). \quad (10)$$

Figure 2 shows a contour plot of E (when $n \to \infty$) as a function of θ and ϕ. When $n \to \infty$, E accounts only for the finite-difference x-y splitting error and can be written as,

$$E = \sqrt{1 - \cos^2\phi \sin^2\theta - \sin^2\phi \sin^2\theta} - \left(\sqrt{1 - \cos^2\phi \sin^2\theta} + \sqrt{1 - \sin^2\phi \sin^2\theta} - 1\right). \quad (11)$$

Clearly, the inline and crossline splitting error increases as the dip angle θ increases, and is largest along the diagonal lines $x = \pm y$ ($\phi = 45$ degrees) when dip θ is fixed. The fact that the phase error varies with azimuth means that waves propagate with different velocities along different azimuth directions, a numerical anisotropy due to the inline and crossline splitting. The anisotropy of wave propagation will cause mispositioning of migrated dipping reflectors and, hence, misleading interpretation of complicated structures. For example, for a reflector dip of 65 degrees, the timing error after one second of downward extrapolation will be 123 ms.

To compensate for the finite-difference errors and yet still retain the efficiency of the splitting method, we need to solve an extra phase-compensation equation at each step of wavefield extrapolation,

$$\frac{\partial P}{\partial z} = \left[\frac{i\omega}{v(x, y, z)} E \right] P. \quad (12)$$

The finite-difference error compensation equation in (12) can be solved using any of several familiar numerical methods used to solve wave equations. The square-root operator in E must be expanded and approximated to a certain order of paraxial equation, if the finite-difference method is to be used. For example, expanding the operator E in equation (8) and ignoring higher-order terms gives the first-order paraxial equation for the error compensation,

$$\frac{\partial P}{\partial z} = -i \left(\sum_{j=1}^{n} 2\alpha_j \beta_j \right) \frac{v^3(x, y, z)}{\omega^3} \frac{\partial^2}{\partial x^2} \frac{\partial^2}{\partial y^2} P. \quad (13)$$

Solving equation (13) using an explicit first-order forward finite-difference scheme along the z-axis will result in an unconditionally unstable solution, because the norm of the transfer function is always greater than or equal to 1. Damping must be applied to ensure stability (Graves and Clayton, 1990), if the explicit scheme is to be used. Implicit

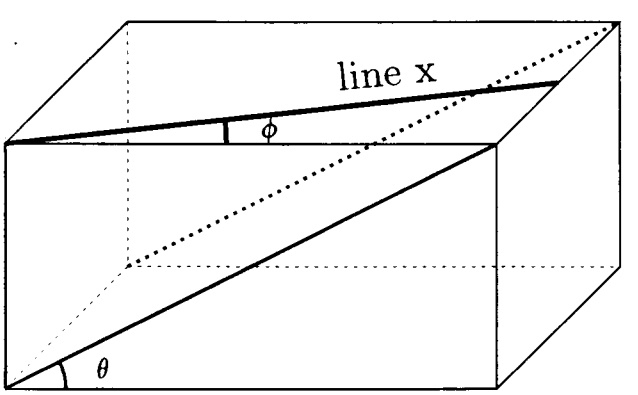

FIG. 1. A 3-D model of a single dipping reflector. The dip angle of the reflector is θ. The azimuth angle between line of interest and dip of reflector is ϕ.

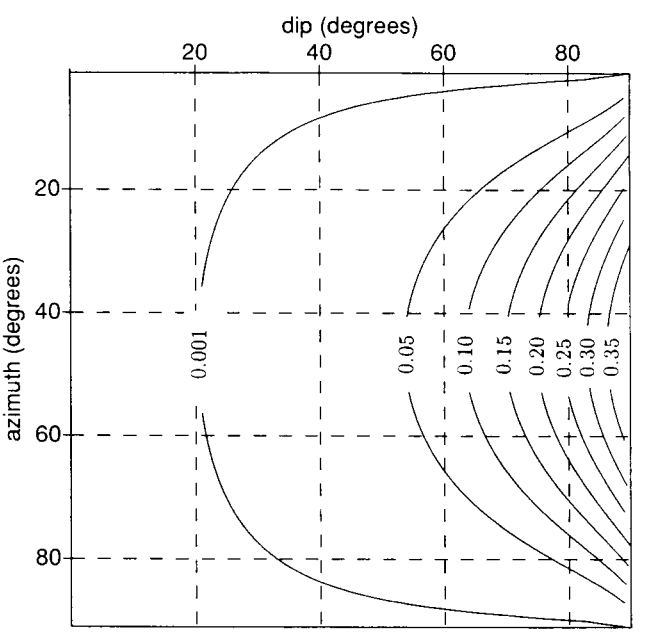

FIG. 2. Contour plot of inline and crossline splitting error. The splitting error is defined as the time error (in seconds) per one second of downward extrapolation.

schemes (without x-y splitting), on the other hand, though unconditionally stable, require relatively heavy computation, which we tried to avoid by using the x-y splitting method to solve equation (4), initially.

Since the error E is small in a single step of wavefield extrapolation, the effect of the compensation process is similar to that of residual migration (Rothman, 1985), in that waves propagate very little in one extrapolation step. Therefore, when lateral velocity variation is moderate, it is reasonable to use a reference velocity $v_a(z)$ (for example, velocity averaged over (x, y)) to replace $v(x, y, z)$ in equation (12) and thus benefit from a phase-shift solution,

$$P(z + \Delta z) = P(z) \exp\left(\frac{i\omega}{v_a(z)} E\Delta z\right). \tag{14}$$

Since a phase-shift operator, which is a linear function of frequency ω, corresponds to a time shift in the time domain, we recognize that E is actually the timing error of the finite-difference splitting for one $\Delta z/v$ (or timing error/1s of downward extrapolation).

It turns out that this approach is similar to that of Kitchenside (1988). Kitchenside implemented the first square-root operator (the 3-D wave equation) in equation (8) with the phase-shift migration using a minimum velocity $v_\alpha(z)$. He then combined the remaining operators in equation (8) [using velocity $v_\alpha(z)$] with the operators in equation (1) (using velocity $v(x, y, z)$) to obtain a residual wavefield extrapolation equation. Instead of using the implicit finite-difference method, he solved the residual wavefield extrapolation equation by the explicit finite-difference method. Since a laterally invariant velocity function is used in implementing the operators in equation (8), naturally, the accurate phase-shift operator is chosen in this approach for every operator in equation (8). This leaves the migration part of solving equation (3) unchanged from the conventional implicit finite-difference method. One major advantage of this approach is that the commonly used, conventional, 3-D finite-difference migration need not be changed and the error compensation only applies as a phase-shift filter at certain depth steps. Both Kitchenside's and this approach will have the accuracy of the phase-shift migration (i.e., with no steep-dip limitation, no x-y splitting error, and no finite-difference dispersion), when velocity is a function of depth only. When velocity varies laterally, both can use Gazdag's method of phase-shift plus interpolation (Gazdag and Sguazzero, 1984) to improve accuracy. However, since the phase-shift method is used to solve the residual phase-error compensation equation (12) while Kitchenside uses the phase-shift method to solve the wave equation (1), the error of this approach, using the phase-shift plus interpolation, will be smaller than that of Kitchenside's when velocity varies laterally (assuming that spatial derivatives of velocity are small). As will be explained later, the residual error compensation can be applied every few depth steps of extrapolation, while the 3-D wave equation in Kitchenside's approach must be solved for every depth step; therefore, this approach is also more efficient.

It is important that all the aspects, including the Crank-Nicholson method (Claerbout, 1985), the finite-difference approximation of derivatives (Claerbout, 1985), and the "1/6 trick" (Claerbout, 1985) of the conventional implicit finite-difference solution to equation (3) be taken into consideration when solving equation (12). If the conventional implicit finite-difference method is used in migration, after some algebra, the solution to equation (12) is given by,

$$P(z + \Delta z) = \exp\left[i\left(k_z - \frac{\omega}{v_a(z)}\right)\Delta z\right] \times \prod_{j=1}^{n} \frac{a_j + ib_j}{a_j - ib_j} \times \prod_{j=1}^{n} \frac{c_j + id_j}{c_j - id_j} \times P(z), \tag{15}$$

where

$$k_z = \sqrt{\left(\frac{\omega}{v_a(z)}\right)^2 - k_x^2 - k_y^2},$$

$$a_j = \frac{1 - \left[\gamma\Delta x^2 + \beta_j\left(\frac{v_a(z)}{\omega}\right)^2\right]\hat{k}_x^2}{\Delta z},$$

$$b_j = \frac{v_a(z)\alpha_j\hat{k}_x^2}{2\omega},$$

$$c_j = \frac{1 - \left[\gamma\Delta y^2 + \beta_j\left(\frac{v_a(z)}{\omega}\right)^2\right]\hat{k}_y^2}{\Delta z}, \tag{16}$$

$$d_j = \frac{v_a(z)\alpha_j\hat{k}_y^2}{2\omega}.$$

In equation (16), γ is the "1/6 trick" value used to improve the accuracy of the second-hand-order finite-difference approximation, with typical γ value of 0.14. Claerbout (1985) defined $\hat{k}_x^2$ and $\hat{k}_y^2$ as approximations to the true lateral wavenumbers that result from the second-order finite difference approximations of the derivative operators $-\partial^2/\partial x^2$ and $-\partial^2/\partial y^2$, respectively, as expressed below,

$$\hat{k}_x^2 = \frac{2 - 2\cos(k_x\Delta x)}{\Delta x^2},$$
$$\hat{k}_y^2 = \frac{2 - 2\cos(k_y\Delta y)}{\Delta y^2}. \tag{17}$$

Figure 3 shows the impulse response of the finite-difference-error compensation operator computed by the phase-shift method for a frequency of 20 Hz and a depth step of 100 m. The operator is anisotropic, with maximum data adjustment along the diagonal lines and no action along either $x = 0$ or $y = 0$ lines. The effective area over which the operator applies becomes smaller as frequency becomes higher and as the depth step becomes smaller. In practice, the error compensation operator need be applied only once every few depth extrapolation steps. Because of the narrowness of the effective width of the operator, a 2-D convolutional method can also be used efficiently to handle lateral velocity variation, but caution must be taken to avoid numerical instability.

The accuracy of using equation (14) with one reference velocity v_a to compensate for the finite-difference splitting errors in the presence of lateral velocity variation is the same as that of using Kitchenside's method. When lateral velocity variation is large, Gazdag's method of phase-shift plus interpolation (Gazdag and Sguazzero, 1984) can be used to solve equation (12). Defining n_a to be the number of reference velocities used to solve equation (14), and A_i and Θ_i to be the amplitude and the phase of the solution $P_i(z + \Delta z)$ to equation (14) using reference velocity v_i, we can then use polynomial interpolation of the n_a individual solutions $P_i(z + \Delta z)$ to obtain the solution $P(z + \Delta z) = A \exp(i\Theta)$ at location (x, y, z),

$$\begin{aligned} \mathbf{A} &= \text{polint}(\mathbf{V}_a^3, \mathbf{A}_a, na, v^3(x, y, z)), \\ \mathbf{\Theta} &= \text{polint}(\mathbf{V}_a^3, \mathbf{\Theta}_a, na, v^3(x, y, z)), \end{aligned} \tag{18}$$

where $\mathbf{V}_a = (v_1(z), v_2(z), \ldots, v_{n_a}(z))$ is the reference velocity vector, $\mathbf{A}_a = (A_1, A_2, \ldots, A_{n_a})$ is the amplitude vector, $\mathbf{\Theta}_a = (\Theta_1, \Theta_2, \ldots, \Theta_{n_a})$ is the phase vector, and polint(X, Y, N, x) is the polynomial interpolation function that returns interpolated function value at x from N data points (X_i, Y_i), $i = 1, N$. The interpolations are performed along the velocity-cubed axis because, as indicated in equation (13), the leading term in the phase error due to the finite-difference splitting is proportional to v^3.

Figure 4 shows the percentage of root-mean-squared (rms) relative phase error (after applying the constant-velocity phase-shift compensation) as a function of percentage of lateral velocity variation along the diagonal line (ϕ = 45 degrees) with dip angle of 45 degrees, for n_a = 1, 3, and 5. The rms relative phase error p_{rms} is defined as

$$p_{\text{rms}} = \sqrt{\frac{1}{(v_{\max} - v_{\min})} \int_{v_{\min}}^{v_{\max}} \left[\frac{p(v) - p_{\text{split}}(v) - p_{\text{comp}}(v)}{p(v)} \right]^2 dv}, \tag{19}$$

where $v_{\max}$ is the maximum velocity, $v_{\min}$ is the minimum velocity, $p(v)$ is the correct phase computed using the wave equation (1), $p_{\text{split}}(v)$ is the phase computed using the splitting equation (7), $p_{\text{comp}}(v)$ is the phase interpolated from the n_a phases computed from the compensation equation (14). The lateral velocity variation v_{lat} is defined as,

$$v_{\text{lat}} = \frac{v_{\max} - v_{\min}}{v_{\min}}. \tag{20}$$

The original phase error using the conventional splitting method, in this case, is 3.53 percent. Therefore, as shown in Figure 4, even for 100 percent lateral velocity variation, the relative phase error is 2.5 percent if only one constant-velocity phase-shift compensation (i.e., without interpolation) is used, which is still a reduction of 30 percent of phase error from the conventional finite-difference splitting method. The relative phase error drops to 0.35 percent, if five reference velocities are used in the phase compensation to give the interpolated phase. Figure 4 helps us determine the number of reference velocities needed for given acceptable phase error and given lateral velocity variation.

In media having strong lateral velocity variation, 3-D migration with this approach has higher accuracy than Gazdag's method of phase shift plus interpolation. The greater accuracy is achieved, because interpolation is applied to the computation of the residual phase error (which is much smaller than the phase itself) in this approach while Gazdag applied interpolation to the computation of the phase. If the compensation is done every 10 depth steps with three reference velocities, the cost of 3-D migration using this method will be that of the conventional 3-D finite-difference migration plus 1/10 of that of three-velocity 3-D phase-shift plus interpolation migration.

IMPLEMENTATION AND EXAMPLES

The 3-D poststack migration downward continues the input CMP stack and obtains the migrated images from the downward extrapolated wavefield at $t = 0$. During each step of downward extrapolation, the first equation in (3) is solved first, and then, the last n equations in (3) are solved sequentially using the x-y splitting method. Every few depth steps, the finite-difference-error compensation equation (12) is solved using the phase-shift method. In the frequency-space domain, one-pass 3-D depth migration with finite-difference-error compensation is implemented as follows.

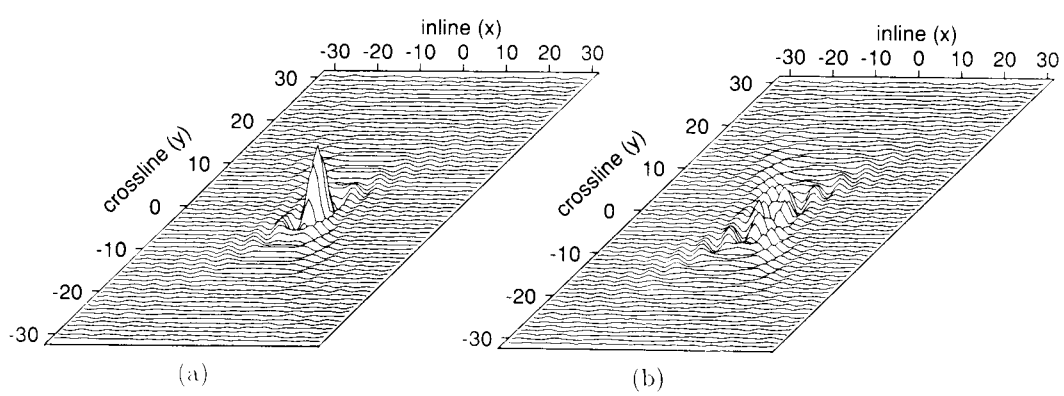

FIG. 3. Impulse response of the finite-difference splitting-error compensation operator for a frequency of 20 Hz and a compensation step of 100 m. Sampling intervals along x, y and z are 12.5 m. Velocity is constant, 2000 m/s, in the model. (a) real part of the response; (b) imaginary part of the response.

input 3-D stack $P(x, y, z = 0, t)$

$FFT[P(x, y, z = 0, t)] = P(x, y, z = 0, \omega)$

$Q(x, y, z, t = 0) = 0.$

for $z = \Delta z, 2\Delta z, \ldots, z_{\max}$

{

for all $x, y, \omega \left\{ P(x, y, \omega) = P(x, y, \omega) \times \exp\left(\frac{i\omega}{v(x, y, z)} \Delta z\right) \right\}$

for all y, ω

{

for $i = 1, n \left\{ \frac{\partial P}{\partial z} = \frac{i\omega}{v(x, y, z)} \frac{\alpha_i S_x}{1 + \beta_i S_x} P \right\}$

}

for all x, ω

{

for $i = 1, n \left\{ \frac{\partial P}{\partial z} = \frac{i\omega}{v(x, y, z)} \frac{\alpha_i S_y}{1 + \beta_i S_y} P \right\}$

}

for certain z steps and all $\omega \left\{ \frac{\partial P}{\partial z} = \frac{i\omega\, E}{v(x, y, z)} P \right\}$

for all $\omega\{Q(x, y, z) = Q(x, y, z) + P(x, y, \omega)\}$

for all $x, y, \omega\{P(x, y, \omega) = P(x, y, \omega) - Q(x, y, z)/n\omega\}$

}

output 3-D migrated data $Q(x, y, z)$

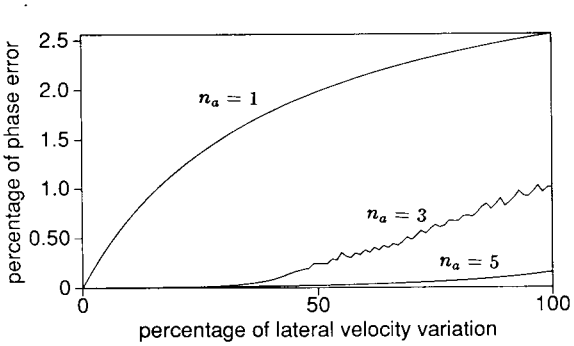

FIG. 4. Percentage of the remaining phase error as a function of percentage of lateral velocity variation for azimuth angle of 45 degrees, and dip angle of 45 degrees, using n_a reference velocities in the finite-difference error compensation.

As seen here, the image is obtained by summing the downward-continued wavefield along the ω-axis, giving the wavefield at $t = 0$. The subtraction of image Q from the downward extrapolated wavefield P in the last step of each downward extrapolation step reduces the FFT wraparound along the time axis (Kjartansson, 1979).

Similarly, implementation of 3-D poststack *forward modeling* in the frequency-space domain is as follows:

input 3-D reflectivity $Q(x, y, z, t = 0)$

$P(x, y, z = 0, \omega) = 0.$

for $z = z_{\max}, z_{\max} - \Delta z, \ldots, \Delta z$

{

for all $x, y, \omega \left\{ P(x, y, \omega) = P(x, y, \omega) \times \exp\left(\frac{i\omega}{v(x, y, z)} \Delta z\right) \right\}$

for all y, ω

{

for $i = 1, n \left\{ \frac{\partial P}{\partial z} = \frac{i\omega}{v(x, y, z)} \frac{\alpha_i S_x}{1 + \beta_i S_x} P \right\}$

}

for all x, ω

{

for $i = 1, n \left\{ \frac{\partial P}{\partial z} = \frac{i\omega}{v(x, y, z)} \frac{\alpha_i S_y}{1 + \beta_i S_y} P \right\}$

}

for certain z steps and all $\omega \left\{ \frac{\partial P}{\partial z} = \frac{i\omega\, E}{v(x, y, z)} P \right\}$

for all $x, y, \omega\{P(x, y, \omega) = P(x, y, \omega) + Q(x, y, z)\}$

}

$FFT^{-1}[P(x, y, z = 0, \omega)] = P(x, y, z = 0, t)$

output 3-D stack $P(x, y, z = 0, t)$

Instead of summing the downward extrapolated wavefield along the frequency axis as when doing the 3-D migration, the reflectivity function Q is added to the upward-continued wavefield P at each depth level to become exploding sources at $t = 0$. The surface-recorded, 3-D poststack data are obtained from the wavefield upward extrapolated to $z = 0$.

Because the finite-difference splitting error in each depth step is small, though cumulative error may be large, the error compensation can be applied every few depth steps of extrapolation to reduce the computational effort of the compensation process. With the compensation step being eight depth-extrapolation steps, tests showed that the error

compensation process increases the total computational cost by about 15 percent.

Figure 5 compares impulse responses of 3-D migration without and with the error compensation. An impulse is placed at $x = y = 0$ and at time $t = 28$ in the input 3-D stack. A migration operator with order $2n = 2$ is used in both tests. As expected, the conventional 3-D migration (without error compensation) gives a result that departs from the ideal — a hemisphere. The depth slices of the conventional approach display a diamond-shape (as opposed to the correct circular response) as a result of the anisotropy of the finite-difference splitting method. Note also the build up of evanescent energy near the center of the impulse response. This evanescent energy becomes dominant at shallow depth slices. With phase-shift implementation of the finite-difference error compensation operator, on the other hand, the 3-D migration gives a more nearly circular and correctly positioned impulse response. Also, as shown in Figure 5, because the phase-shift method propagates only the nonevanescent energy, the error compensation has the additional advantage of suppressing evanescent energy generated by the finite-difference implementation. Furthermore, the accuracy of imaging steep dips is improved to 90 degrees, as shown in Figure 5b, since the velocity in the model is constant.

Figure 6 compares impulse responses of 3-D modeling without and with finite-difference error compensation. An impulse is specified at $x = y = 0$ and at $z = 12$ in the input 3-D reflectivity model. Again the paraxial equation of order $2n = 2$ is used in both cases. Figures 6(a) and 6(b) show the diffractions generated with the two approaches along the diagonal line $x = y$. The error in arrival time of the diffraction at the edges is as large as about 10 time samples, though the total traveltime is about 45 time samples; a relative error of more than 20 percent! With the finite-difference-error compensation, the impulse response of the 3-D modeling is more accurate and has less evanescent energy present than does that of the conventional approach.

A more geologically plausible model is tested and results are shown in Figure 7. The model has four reflectors, with the medium velocity varying linearly with depth, $v(z) = 1500 + 2\ z$(m/s). The first reflector is an upward hemisphere truncated with a horizontal bed. The strikes of the two dipping interfaces, with dips of 45 degrees and 60 degrees, respectively, are perpendicular to the diagonal line $x = y$. Both dipping interfaces are truncated with horizontal beds. The fourth reflector is simply horizontal. The 3-D phase-shift method is used in forward modeling of the wave field. The 3-D frequency-space depth migration of order $2n = 2$ without and with finite-difference-error compensation is applied to the 3-D stack. Figure 7 displays six rows of pictures, with four pictures in each row. The pictures in each row, in order, are the reflector model, 3-D phase-shift modeling, conventional 3-D frequency-space depth migration without error compensation, and 3-D frequency-space depth migration with error compensation. The migration with the compensation gives more accurate images and higher dip accuracy of the hemisphere than does the migration without the compensation as shown in Figures 7(b), 7(c), and 7(e). In Figure 7(d), vertical sections at $x = 0$ show that the 60-degree dipping reflector is undermigrated and weakened in the migration without the compensation. The anisotropy of the 3-D migration due to the inline and crossline splitting gives the diamond-shape image of the original circle on the depth slice of migrated 3-D data, as shown in Figure 7(c). The anisotropic error is suppressed by the error compensation process.

CONCLUSION

The accuracy of conventional one-step, x-y splitting, 3-D depth migration, and modeling can be improved by doing the finite-difference error compensation during the wavefield extrapolation. When lateral velocity variation is moderate, the compensation can be simply done using the phase-shift method. The modified 3-D wavefield extrapolation method retains most of the efficiency of the splitting approach, yet improves accuracy of positioning of steep-dip events and reduces undesirable dispersion and evanescent energy in the conventional 3-D wavefield extrapolation method.

The phase-shift plus interpolation method, or other numerical methods, such as the 2-D convolutional method with a stable convolution operator, must be used to solve the compensation equation, when strong lateral velocity variations are present.

ACKNOWLEDGMENTS

This work benefits from many discussions with Dave Hale and Ken Larner at Colorado School of Mines. Review and suggested revisions of the paper by Dave Hale, Ken Larner, Jack Cohen, and Norm Bleistein are greatly appreciated. Comments from Wendell Wiggins, Ron Chambers, and Alfonso Gonzalez-Serrano at Western Geophysical were also helpful. Thanks for financial support are due to the sponsors of the Consortium Project on Seismic Inverse methods for Complex Structures at the Center of Wave Phenomena of Colorado School of Mines and the U.S. Dept. of Energy, Grant Number DE-FG02-89ER14079.

REFERENCES

Brown, D. L., 1983, Applications of operator separation in reflection seismology: Geophysics, **48**, 288–294.
Claerbout, J. F., 1985, Imaging the earth's interior: Blackwell Scientific Publications, Inc.
Gazdag, J., 1978, Wave-equation migration with the phase-shift method: Geophysics, **43**, 1342–1351.
Gazdag, J., and Sguazzero, P., 1984, Migration of seismic data by phase-shift plus interpolation: Geophysics, **49**, 124–131.
Graves, R. W., and Clayton, R. W., 1990, Modeling acoustic waves with paraxial extrapolators: Geophysics, **55**, 306–319.
Hale, D., 1990, 3-D depth migration via McClellan transformations: 60th Ann. Internat. Mtg. Soc. of Expl. Geophys., Expanded Abstracts, 1325–1328.
Kitchenside, P., 1988, Steep dip 3-D migration: Some issues and examples: 58th Ann. Internat. Mtg. Soc. Expl. Geophys., Expanded Abstracts, 976–978.
Kjartansson, E., 1979, Attenuation of seismic waves in rocks and applications in energy exploration: Ph.D. thesis, Stanford Univ.
Lee, M., and Suh, S., 1985, Optimization of one-way equation: Geophysics, **50**, 1634–1637.
Ma, Z., 1982, Finite-difference migration with higher-order approximation: Oil Geophys. Prosp., **17**, 6–15.
Ristow, D., 1980, 3-D downward extrapolation of seismic data in particular by finite difference method: Ph.D. thesis, Univ. of Utrecht, The Netherlands.
Rothman, D., Levin, S., and Rocca, F., 1985, Residual migration: Application and limitations: Geophysics, **50**, 110–126.
Yilmaz, O., 1987, Seismic data processing: Society of Exploration Geophysicists.

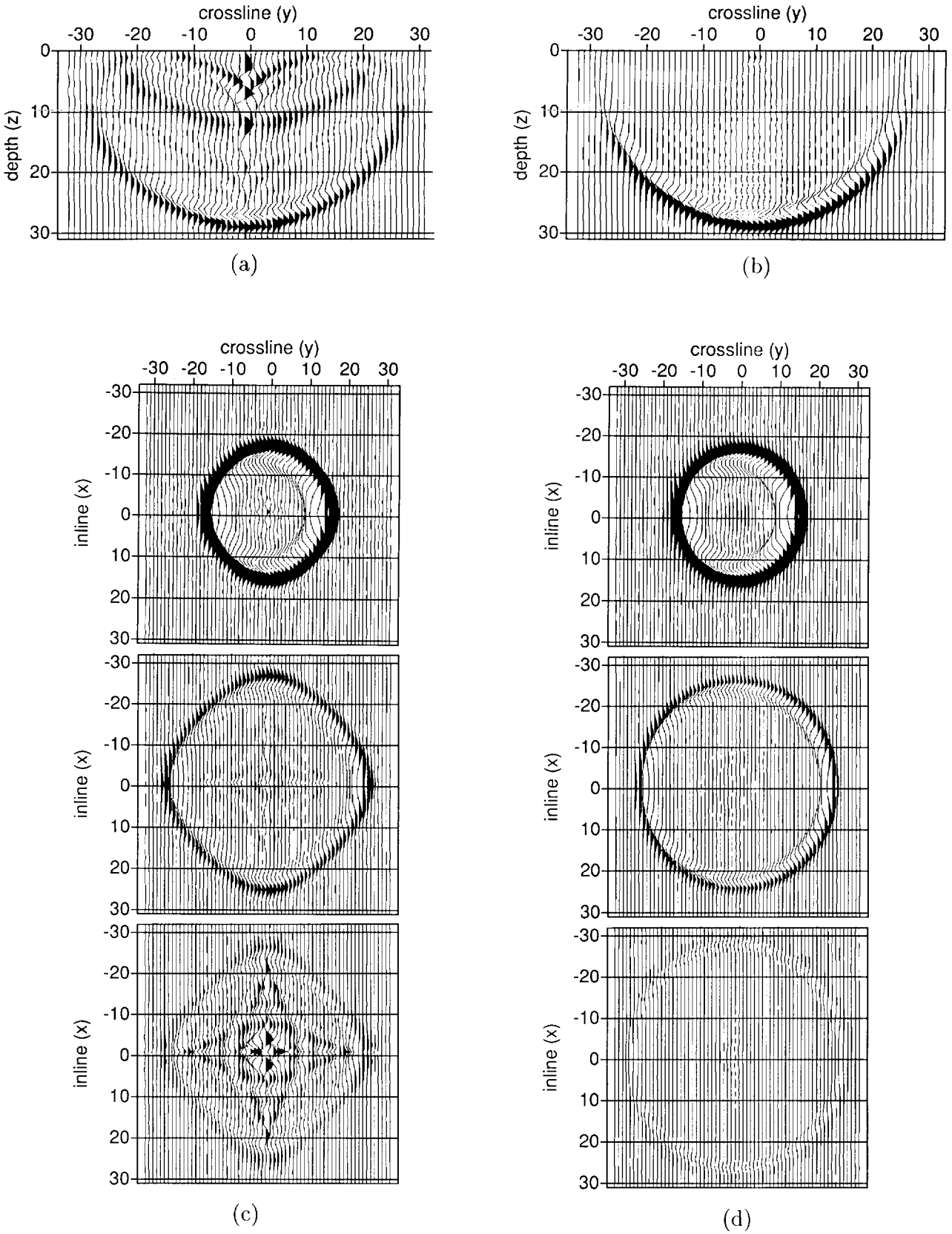

FIG. 5. Comparison of impulse responses of 3-D migrations without [(a) and (c)] and with [(b) and (d)] the finite-difference error compensation. Sampling intervals along x, y, z and t are 1, with constant velocity $v = 2$, in the computation. A 65-degree extrapolation operator is used in both cases. (a) and (b): vertical section at $x = 0$; (c) and (d): depth slices at $z = 25$, $z = 15$, and $z = 5$.

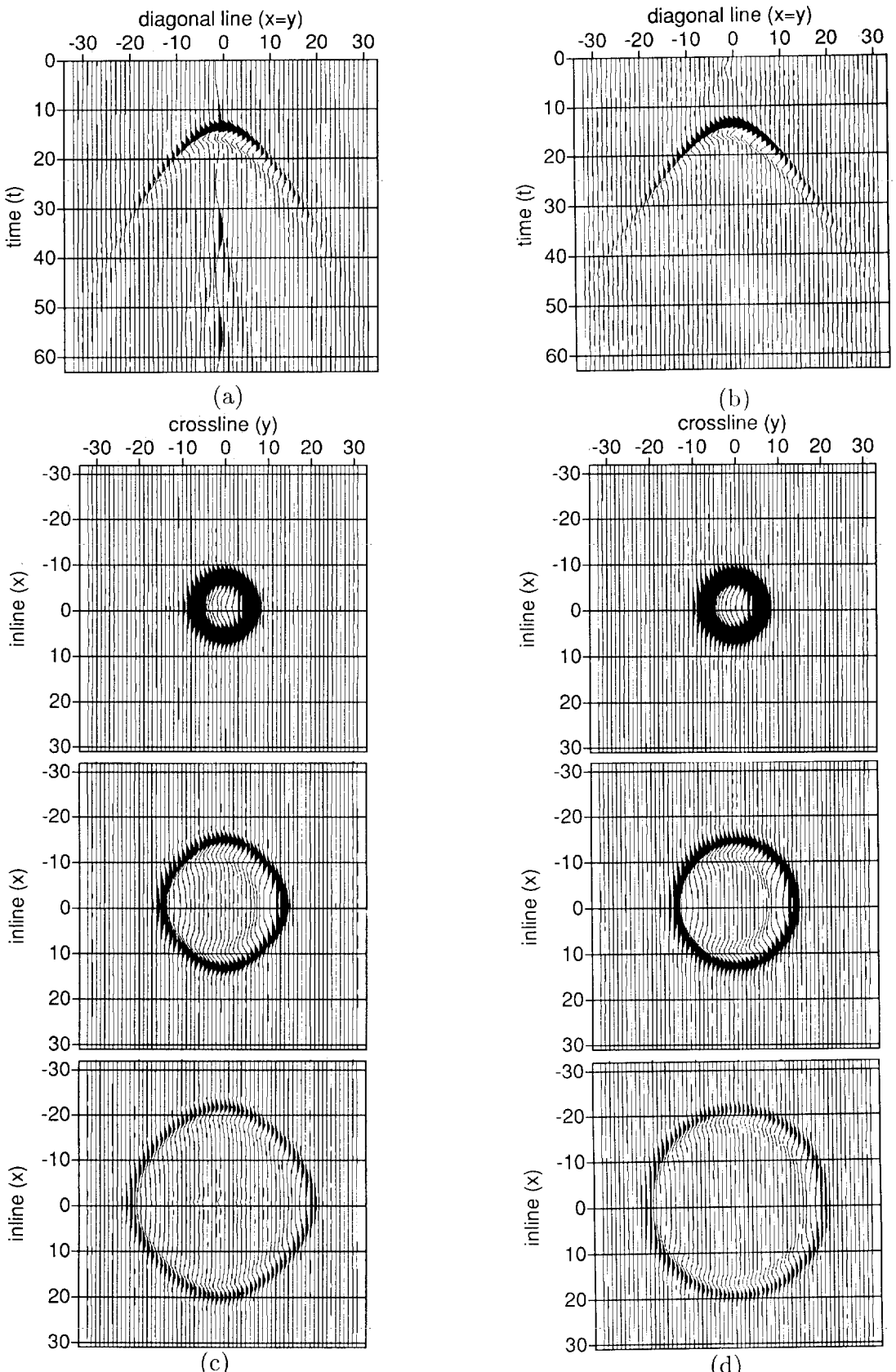

FIG. 6. Comparison of impulse responses of 3-D modeling without [(a) and (c)] and with [(b) and (d)] the finite-difference error compensation. Sampling intervals along x, y, z and t are 1, with constant velocity $v = 2$, in the computation. A 65-degree extrapolation operator is used in both cases. (a) and (b): vertical section at diagonal line $x = y$. The error is maximum along $x = \pm y$ lines. The timing errors of the diffraction at both edges in (a) are as large as 10 samples. (c) and (d): time slices at $t = 15$, $t = 20$, and $t = 25$.

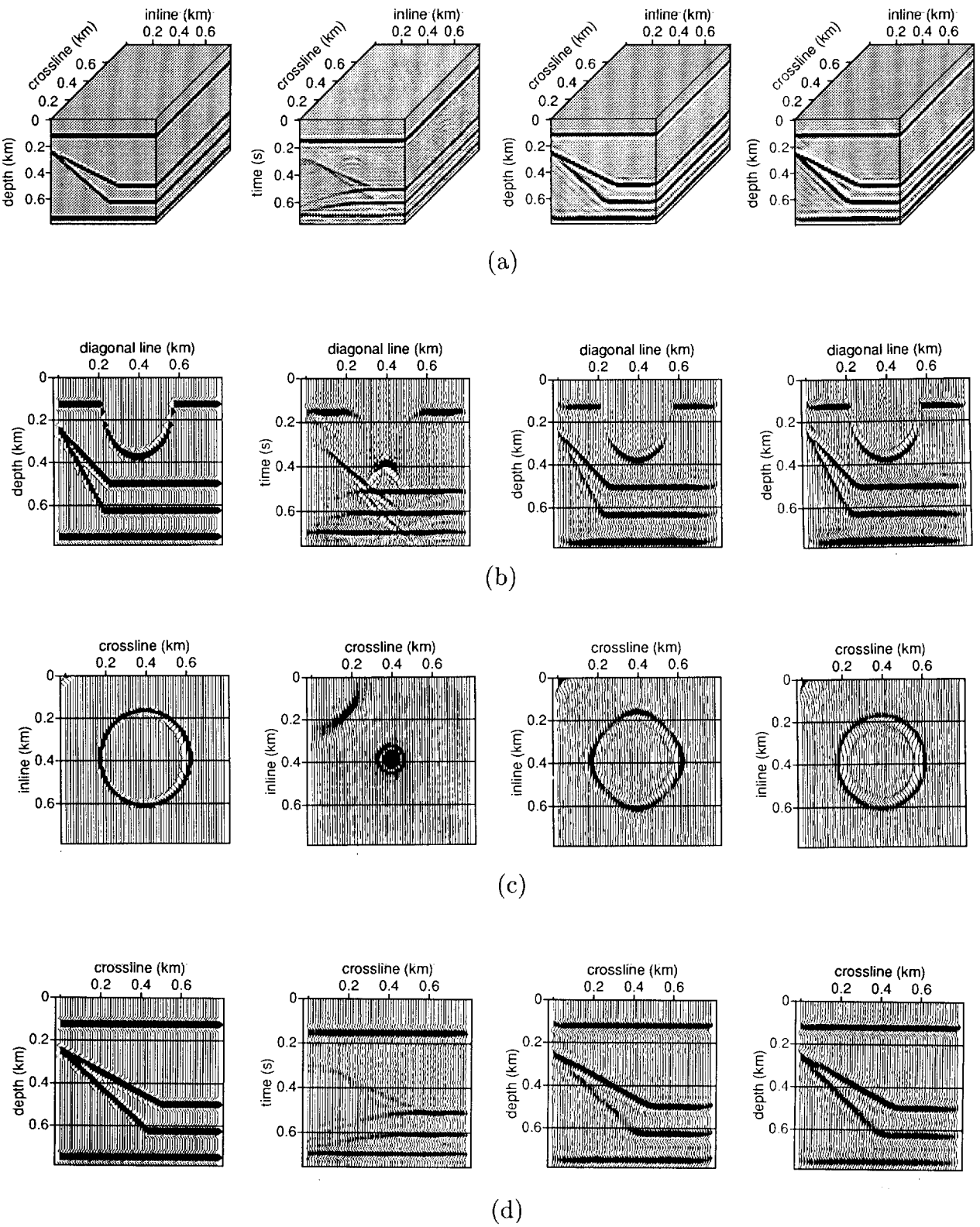

FIG. 7. Comparison of 3-D migration without and with the finite-difference error compensation. Each row in Figure 7 shows, in order, the reflector model, 3-D phase-shift modeling, migration without the compensation, and migration with the compensation. (a) Cube displays. (b) Vertical sections along the diagonal line $x = y$. (c) Depth slices at $z = .25$ km and time slice at $t = 0.40$ s. (d) Vertical sections at $x = 0$. *(continued)*

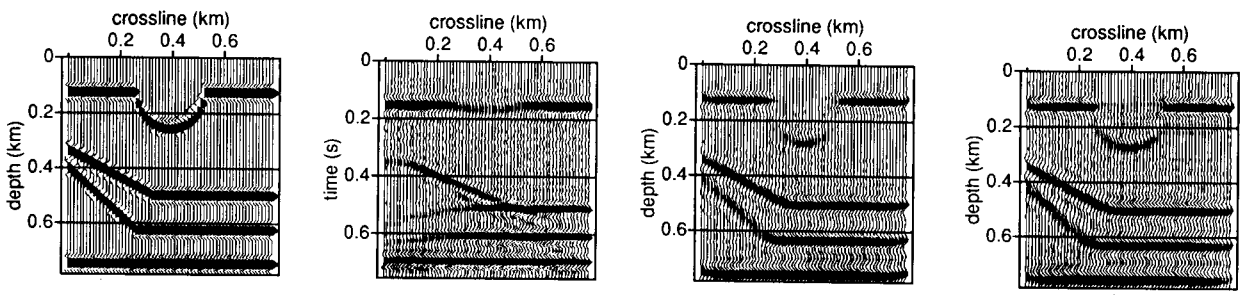

(e)

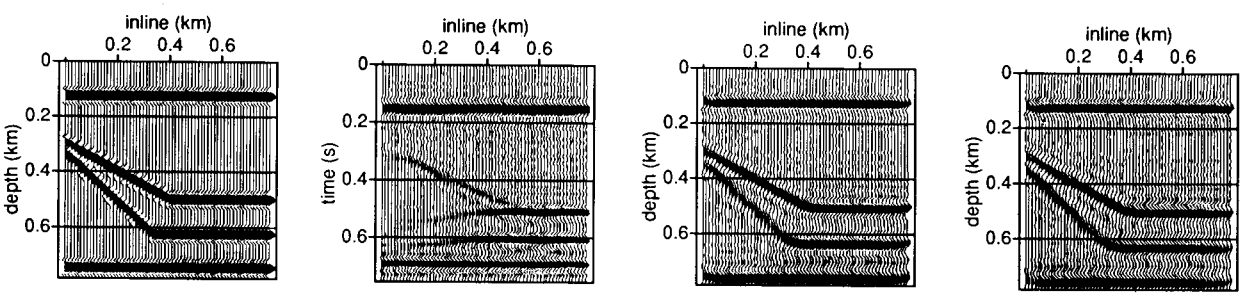

(f)

FIG. 7. *continued*. (e) Vertical sections at $y = 0.175$ km. (f) Vertical sections at $y = 0.10$ km.